BRAIN
ORIGINAL ARTICLE

Bi-allelic loss-of-function OBSCN variants predispose individuals to severe recurrent rhabdomyolysis

Macarena Cabrera-Serrano,[1,2,3] Laure Caccavelli,[4] Marco Savarese,[5] Anna Vihola,[5,6] Manu Jokela,[7,8] Mridul Johari,[5] Thierry Capiod,[4] Marine Madrange,[4] Enrico Bugiardini,[9] Stefen Brady,[10] Rosaline Quinlivan,[11] Ashirwad Merve,[11] Renata Scalco,[11] David Hilton-Jones,[12] Henry Houlden,[9] Halil Ibrahim Aydin,[13] Serdar Ceylaner,[14] Sarah Drewes,[15] Jerry Vockley,[16] Rhonda L. Taylor,[1,2] Chiara Folland,[1,2] Aasta Kelly,[1] Hayley Goullee,[1,2] Emil Ylikallio,[17,18] Mari Auranen,[17] Henna Tyynismaa,[18,19] Bjarne Udd,[5,6] Alistair R. R. Forrest,[1,2] Mark R. Davis,[20] Drago Bratkovic,[21] Nicholas Manton,[22] Thomas Robertson,[23] Cullen O'Gorman,[24] Pamela McCombe,[24,25] Nigel G. Laing,[1,2,20] Liza Phillips,[22,26] Pascale de Lonlay[4] and Gianina Ravenscroft[1,2]

Rhabdomyolysis is the acute breakdown of skeletal myofibres in response to an initiating factor, most commonly toxins and over exertion. A variety of genetic disorders predispose to rhabdomyolysis through different pathogenic mechanisms, particularly in patients with recurrent episodes. However, most cases remain without a genetic diagnosis. Here we present six patients who presented with severe and recurrent rhabdomyolysis, usually with onset in the teenage years; other features included a history of myalgia and muscle cramps. We identified 10 bi-allelic loss-of-function variants in the gene encoding obscurin (*OBSCN*) predisposing individuals to recurrent rhabdomyolysis. We show reduced expression of *OBSCN* and loss of obscurin protein in patient muscle. Obscurin is proposed to be involved in sarcoplasmic reticulum function and Ca^{2+} handling. Patient cultured myoblasts appear more susceptible to starvation as evidenced by a greater decreased in sarcoplasmic reticulum Ca^{2+} content compared to control myoblasts. This likely reflects a lower efficiency when pumping Ca^{2+} back into the sarcoplasmic reticulum and/or a decrease in Ca^{2+} sarcoplasmic reticulum storage ability when metabolism is diminished. *OSBCN* variants have previously been associated with cardiomyopathies. None of the patients presented with a cardiomyopathy and cardiac examinations were normal in all cases in which cardiac function was assessed. There was also no history of cardiomyopathy in first degree relatives, in particular in any of the carrier parents.
This cohort is relatively young, thus follow-up studies and the identification of additional cases with bi-allelic null *OBSCN* variants will further delineate *OBSCN*-related disease and the clinical course of disease.

1 Harry Perkins Institute of Medical Research, Nedlands, WA, Australia
2 Centre of Medical Research, University of Western Australia, Nedlands, WA, Australia
3 Unidad de Enfermedades Neuromusculares. Servicio de Neurologia y Neurofisiologia, Hospital Virgen del Rocio, Sevilla, Spain
4 Inserm U1151, Institut Necker Enfants-Malades, Reference Center of Inherited Metabolic Diseases and MetabERN, Necker-Enfants-Malades Hospital, Paris University, Paris, France
5 Folkhälsan Research Center, Helsinki, Finland and Department of Medical Genetics, Medicum, University of Helsinki, Helsinki, Finland

Received June 04, 2021. Revised December 04, 2021. Accepted December 10, 2021. Advance access publication December 24, 2021

6 Tampere Neuromuscular Center, Tampere University Hospital, Tampere, Finland
7 Neuromuscular Research Center, Department of Neurology, Tampere University and University Hospital, Tampere, Finland
8 Neurocenter, Department of Neurology, Clinical Neurosciences, Turku University Hospital and University of Turku, Turku, Finland
9 Department of Neuromuscular Disorders, UCL Queen Square Institute of Neurology, London, UK
10 Department of Neurology, Southmead Hospital, Bristol, UK
11 MRC Centre for Neuromuscular Diseases, University College Hospitals, London, UK
12 Neurosciences Group, Nuffield Department of Clinical Neurosciences, Weatherall Institute of Molecular Medicine, University of Oxford, Oxford, UK
13 Department of Pediatrics, Baskent University, Ankara, Turkey
14 Intergen Genetic Diagnosis and Research Center, Ankara, Turkey
15 UPMC Children's Hospital of PittsburghPittsburgh, Pennsylvania, USA
16 University of Pittsburgh School of Medicine, Pittsburgh, Pennsylvania, USA
17 Clinical Neurosciences, Neurology, University of Helsinki and Helsinki University Hospital, Helsinki, Finland
18 Stem Cells and Metabolism Research Program, Faculty of Medicine, University of Helsinki 00290 Helsinki, Finland
19 Neuroscience Center, Helsinki Institute of Life Science, University of Helsinki, Helsinki, Finland
20 Department of Diagnostic Genomics, PathWest Laboratory Medicine WA, Nedlands, WA, Australia
21 Metabolic Clinic, Women and Children's Hospital, North Adelaide, SA, Australia
22 SA Pathology, Women and Children's Hospital, North Adelaide, SA, Australia
23 Anatomical Pathology, Queensland Pathology, Brisbane, Queensland, Australia
24 Centre for Clinical Research, The University of Queensland Centre for Clinical Research, Brisbane, Queensland, Australia
25 Department of Neurology, Royal Brisbane and Women's Hospital, Brisbane, Queensland, Australia
26 The University of Adelaide, Adelaide, SA, Australia

Correspondence to: Dr Gina Ravenscroft
Harry Perkins Institute of Medical Research
6 Verdun St, Nedlands
Western Australia, Australia, 6009
E-mail: gina.ravenscroft@uwa.edu.au

Keywords: rhabdomyolysis; hyperCKaemia; myalgia; exercise intolerance; obscurin

Abbreviations: MNV = multinucleotide variant; SR = sarcoplasmic reticulum

Introduction

Rhabdomyolysis is a serious medical condition involving the rapid breakdown of damaged or injured skeletal myofibres and may require intensive care management. Muscle breakdown results in release of myofibrillar content into the extracellular space and the circulation, resulting in hyperCKaemia (hyperCK) and myoglobinuria. Clinically, rhabdomyolysis can range from asymptomatic episodes with isolated hyperCK to a life-threating condition with profound myoglobinuria, often progressing to acute renal failure and requiring intensive care management in severe cases. Clinical features include acute muscle weakness, myalgia, muscle swelling and elevated creatine kinase (CK) (defined as >5-times the upper normal limit).[1] Some patients also develop compartment syndrome necessitating fasciotomy.

Rhabdomyolysis can be acquired (trauma, ischaemia, infection and toxin or drug-related)[2] or genetic[3] in origin. A fascinating history of rhabdomyolysis exists in the literature, with reports dating back to biblical times and antiquity often in relation to poisoning.[4] Quail poisoning is a well documented cause of rhabdomyolysis and is caused by ingestion of toxins associated with quail meat.[4]

A schema has been suggested to discern rhabdomyolysis cases with a likely genetic contribution.[5] This has an acronym of RHABDO (Recurrent episodes, HyperCK for a prolonged period, Accustomised physical activity, Blood CK >50×UNL, Drug/medication insufficient to explain severity, Other family members affected/Other symptoms).[5] A large single-centre study showed that the most common triggers of rhabdomyolysis included ischaemia/anoxia and traumatic muscle injury in non-neuromuscular cases; whilst in >50% of cases with a known or suspected neuromuscular basis the trigger was exercise.[5]

There is a growing list of Mendelian gene defects associated with increased susceptibility to rhabdomyolysis, including a number of genes involved in muscle metabolism and mitochondrial function.[3,6] Recessive variants in the lipin-1 gene (*LPIN1*) are a common cause of childhood-onset and severe rhabdomyolysis, sometimes resulting in kidney failure and cardiac arrhythmia.[7,8] Impaired synthesis of triglycerides and membrane phospholipids have been hypothesized to underlie the pathogenesis of *LPIN1*-mediated rhabdomyolysis.

More recently, variants in genes encoding structural muscle proteins have been implicated in rhabdomyolysis. Bi-allelic variants in the gene encoding muscular LMNA-interacting protein (*MLIP*) have been shown to underlie a myopathy characterised by mild muscle weakness, myalgia, susceptibility to rhabdomyolysis and persistently elevated basal CK.[9] Further, Alsaif *et al.*[10] have reported a single case of rhabdomyolysis associated with a homozygous missense variant in *MYH1*, the gene encoding myosin heavy chain 2X, and a *MYH1* missense variant is strongly associated with non-exertional rhabdomyolysis in Quarter horses.[11]

In addition, variants in known muscular dystrophy genes can also predispose a patient to rhabdomyolysis; in some cases rhabdomyolysis can be the presenting symptom of an underlying muscular dystrophy, e.g. *ANO5*, *CAV3 DMD*, *FKRP* and *SGCA*[5,6,12–15] or neurogenerative disease, e.g. *TANGO2*.[5]

Variants in *RYR1* encoding the skeletal muscle Ca^{2+} release channel (Ryr1) of the sarcoplasmic reticulum (SR) have been increasingly recognised as an underlying cause of rhabdomyolysis.[16,17] Similarly, likely pathogenic variants in genes critical to excitation-contraction coupling and Ca^{2+} handling (*CACNA1S* and *SCN4A*) have been implicated in exertional heat illness and rhabdomyolysis.[5,18] Kruijt *et al.*[5] identified an underlying genetic diagnosis in 72 of 193 (37%) rhabdomyolysis probands that fulfilled one or more of the RHABDO criteria, these included variants in 22 disease genes. Despite sequencing of known rhabdomyolysis genes, including via large gene panels and exome sequencing, many individuals who experience rhabdomyolysis remain without a definitive genetic diagnosis.[5,19–22]

Identification of the genetic cause in a patient with rhabdomyolysis is important because it enables appropriate advice on how to minimize future episodes, optimized clinical management and genetic counselling.

Obscurin is a component of the sarcomere and localises to the M-band and Z-disks.[23] Obscurin interacts with titin, myomesin and small ankyrin 1 and is proposed to serve as a linker protein between the sarcomere and SR.[24–26] Obscurin is also thought to be involved in SR function and Ca^{2+} regulation.[27,28] *Obscn* null (*Obscn*$^{-/-}$) mice display a mild myopathy, including exercise-induced sarcomeric and sarcolemmal defects.[27–30] Increased susceptibility of obscurin-deficient muscle to damage may trigger bouts of rhabdomyolysis in humans.

In this study we identified six patients with onset of severe recurrent rhabdomyolysis from 12–27 years of age and bi-allelic loss-of-function variants in the obscurin gene (*OBSCN*). Four of the six probands experienced rhabdomyolysis following exercise. Some patients had a history of myalgia and muscle cramps that preceded the initial episode of rhabdomyolysis. Between episodes, CK levels are normal to mildly elevated. We showed reduced *OBSCN* transcript expression and protein abundance in muscle biopsies from affected individuals. Studies of patient cultured myoblasts showed that starvation condition induces aberrant Ca^{2+} flux into the SR and higher levels of myoblast death under basal conditions, the hallmarks of the rhabdomyolysis.[31]

Our data clearly demonstrate that bi-allelic loss-of-function *OBSCN* variants predispose individuals to severe recurrent rhabdomyolysis. *OBSCN* variants should be considered in the diagnosis of patients with recurrent rhabdomyolysis.

Materials and methods

All studies were approved by the Human Research Ethics Committee of the recruiting centre and all individuals participating in this study gave informed consent. Matching of cases was achieved via ongoing collaborations and was also facilitated by Metab-L.[32]

Clinical investigations

Patient details and investigations

We have clinically characterised six probands from six unrelated families originating from Australia ($n = 2$), Finland, Turkey, the UK and the USA. Patients presented with severe rhabdomyolysis, from their teenage years. We performed pedigree analysis, neurological examination, including muscle strength evaluation according to the Medical Research Council (MRC) grading scale, serum CK levels during acute episodes and between episodes (baseline), lower limb muscle MRI and cardiac investigations in some cases, muscle biopsy and genetic workout in the probands and additional family members. The study was approved by the ethics committees of the participating institutions. Sample collection was performed after written informed consent from the patients according to the Declaration of Helsinki.

Muscle pathology

Muscle biopsies were performed in all probands as part of routine diagnostic investigations. The samples were frozen in liquid nitrogen-chilled isopentane and processed for routine histological and histochemical techniques. Muscle samples were also collected for electron microscopy. Processing of muscle for light and electron microscopy was performed as outlined previously.[33]

Genetic investigations

AUS1

DNA from the proband was run on version 1 of a custom designed neuromuscular disease targeted gene panel at Diagnostic Genomics, PathWest, as detailed in Beecroft *et al.*[22] This did not identify any likely pathogenic variants. Whole exome sequencing was then performed using the Ion Proton™ (Ampliseq chemistry, Life Technologies). Variant calling was performed using Torrent Suite V3.6.2. Data were annotated and filtered using an ANNOVAR annotation software suite. Pathogenicity predictions were made using online prediction software programs: SIFT, PolyPhen-2, and MutationTaster.

AUS2

DNA from the proband was sequenced on version 2 the PathWest neuromuscular disease gene targeted panel.[22] No likely causative variants were identified. DNA was subsequently resequenced on version 5 of the panel, which had been updated to include recently identified skeletal muscle disease genes, including *OBSCN*. All mapping and calling of variants was done by the BWA Enrichment App v2.1.2 on the Illumina Basespace Sequence Hub using our custom bed files. Data were analysed in Alissa Interpret (Agilent).

FIN1

Exome sequencing was performed on DNA from the proband as previously described,[34] and was analysed as a clinical exome that did not identify pathogenic variants in genes with previous disease associations in OMIM or ClinVar databases. This patient subsequently underwent targeted resequencing using the MYOcap gene panel.[35]

TUR1

Exome enrichment was performed using Twist Comprehensive Human Exome kit according to manufacturer's instructions. Prepared library was sequenced on MGI DNBSEQ-G400 at 80–100× on-target depth with 150 bp paired-end sequencing at Intergen Genetic Diagnostic Centre (Ankara, Turkey). Bioinformatics analyses were performed using in-house developed workflow derived from GATK best practices at Intergen Genetic Diagnostic Centre.

UK1

Exome sequencing and analysis was performed on the proband's DNA as outlined previously.[36]

USA1

Clinical exome sequencing was performed on the proband at GeneDX. No known or candidate pathogenic variants were identified. Re-examination of the exome in light of the association of *OBSCN* with recurrent rhabdomyolysis, identified a single heterozygous essential splice-site variant in *OBSCN*. DNA from USA1 was subsequently sequenced on version 3 of the PathWest neuromuscular disease gene panel. A second nonsense variant was identified in this individual, by the PathWest panel.

Bi-directional Sanger sequencing was used to confirm the *OBSCN* variants identified and where familial DNA samples were available, to examine segregation of the variants.

Skeletal muscle RNA-sequencing

Skeletal muscle RNA-seq data from a cohort of individuals were studied. These individuals included 30 patients with skeletal muscle disease, four patients with isolated hyperCK and one asymptomatic relative of a skeletal muscle disease proband. We utilized RNA-seq data that were generated using a ribodepletion method, to negate potential bias associated with RNA-sequencing of large genes, including obscurin, in samples generated with a poly-A RNA capture method.[37]

RNA was extracted with Qiagen RNeasy Plus Universal Mini Kit (Qiagen) according to the manufacturer's instructions. The strand-specific RNAseq library was prepared using the Illumina Ribo-Zero Plus rRNA Depletion Kit (Illumina) at the Oxford Genomics Center, Welcome Trust Institute, Oxford, UK. Sequencing was performed on Novaseq (Illumina), generating over 80 million 150bp-long reads per sample. Trimmed sequences were mapped against the hg19 human reference genome using STAR 2.7.0d.

To evaluate *OBSCN* exon usage, we analysed pooled junction data from the 35 RNA-seq experiments.

Quantitative PCR

RNA was extracted from 30 mg frozen tissue using the RNeasy Fibrous Tissue Mini Kit (Qiagen) as described by the manufacturer. RNA was quantified with a Nanodrop ND 1000 spectrophotometer (Thermo Fisher Scientific) and electrophoresed on a 1% agarose gel to confirm RNA integrity and absence of genomic DNA contamination. The SuperScript III First-Strand Synthesis System (Thermo Fisher Scientific) was used to synthesize cDNA from up to 1 μg total RNA using random hexamers according to the manufacturer's protocol. Prior to qPCR, all cDNA's were diluted to the equivalent starting input of 100 ng RNA with UltraPure water (Thermo Fisher Scientific). The Rotor-Gene SYBR Green PCR Kit (Qiagen) was used to set up 10 μl reactions containing 1 μl diluted cDNA and 0.8 μM each of forward and reverse primers (*OBSCN*, *RYR1*, *ACTA1*, *MYOG*, *TBP*, *EEF2*; Supplementary Table 1). Primers were designed to amplify transcript variants 1 (NM_052843.4, isoform A), 2 (NM_001098623.2, isoform B), 3 (NM_001386125.1) and IC (NM_001271223.2, inferred complete isoform). There were no predicted off-target products. There are two long non-coding RNA genes that overlap *OBSCN* and the primers do not amplify these. Primer efficiency (in the range 0.9–1.1) was validated by standard curve. Thermal cycling was performed on the Rotor-Gene Q real-time PCR cycler and data were analysed with the associated software (Qiagen) using a cycle threshold of 0.03. Data were normalized to the geometric mean of two endogenous control genes (*TBP*, *EEF2*) using the delta-Ct method. Graphed data represent the mean ± standard error of the mean (SEM) and were generated using GraphPad Prism (V6.02).

Western blotting

Frozen muscle biopsies were homogenized in modified Laemmli sample buffer, as described previously.[38] Samples were run in Bio-Rad Criterion 3–8% tris-acetate gradient gels (Bio-Rad Laboratories) at room temperature, 100 V, for 4 h. The proteins were transferred from gels onto PVDF membranes with a Bio-Rad TransBlot Turbo device (program Standard SD, 60 min), using discontinuous buffer system, gel/anode buffer 1× CAPS with 0.1% SDS; PVDF/cathode buffer 1× CAPS. Subsequently, the post-blotting gels were stained with Coomassie Brilliant Blue, and the PVDF membranes were incubated in primary antibody solution, rabbit anti-obscurin ob59 (1:800 dilution) overnight at 8°C (anti-obscurin domain 59 antibody is a gift from Prof. Mathias Gautel). Membranes were incubated with HRP-conjugated secondary antibody and the bands were detected using ECL (SuperSignal West Femto, Thermo Fisher Scientific) and ChemiDoc MP digital imager (Bio-Rad). Coomassie-stained gels were used to visualize titin and nebulin bands which served as size markers and loading controls.

Cell-based assays

Immunofluorescence microscopy

Primary myoblasts were fixed and stained as previously described[39] with anti-calnexin primary antibody (clone AF18, refsc-23954, Santa Cruz Biotechnology). Images were acquired on a confocal Leica LSM700 microscope, equipped with a 63× and a 1.3 numerical aperture (NA) oil immersion objective. Quantification and morphological analysis of endoplasmic reticulum was done with Icy v1.9.5.1 (BioImage Analysis Unit, Institut Pasteur, France).

Ca^{2+} measurements

Thapsigargin-induced responses were monitored in a FDSSμCell microplate reader (Hamamatsu Photonics) to assess SR Ca^{2+} content. Myoblasts were plated in 96-well plates at a density of 15 000 cells per well and incubated for 1 h in Earle's Balanced Salt Solution (EBSS) or in complete HAMF10 medium. Myoblasts were loaded with 4 μM Cal-520-AM (AAT Bioquest) for 45 min then washed in recording medium containing (mM) NaCl 116, KCl 5.6, $MgCl_2$ 1.2, HEPES 20 (pH 7.3) and 150 μM EGTA. Thapsigargin (1 μM) was simultaneously added in the absence of external Ca^{2+} in all wells. Recordings were performed at 37°C, frequency acquisition was 1 Hz and fluorescence signals (F) calibrated by adding 50 μM digitonin containing 6 mM Ca^{2+} (final concentrations) to obtain maximal fluorescence signals (F_{max}). Data were expressed as F/F_{max} and SR Ca^{2+} content areas of the TG-evoked responses calculated using Origin software (OriginLab Corp). Thapsigargin was purchased from Alomone Labs and all other reagents were from Sigma-Aldrich.

Apoptosis measurements

Myoblasts were plated in 96-well plates at a density of 5000 myoblasts per well. Caspase 3/7 green apoptosis assay reagent and NuncLight red reagent for nuclear labelling (ref C10423 and 4717,

Essen Biosciences Ltd) were added in each individual well at a 1/1000 final dilution. Four phase images and four fluorescent images per well (excitation 440–480 nm; emission 504–544 nm and excitation 655 nm; emission 681 nm) were taken using IncuCyte® S3 Life Cell Analysis System (Essen Biosciences Ltd). Single green events representing caspase 3/7-positive myoblasts were counted and myoblast number was assessed from nuclear counts.

Statistical analysis

Statistical analysis was performed with GraphPad Prism software using a Mann-Whitney test for all image analysis experiments, Ca^{2+} and apoptosis measurements.

Data availability

The data that support the findings of this study are available from the corresponding author, upon request.

Results

Clinical findings

Here we report six isolated patients presenting with a clinical picture of severe, recurrent rhabdomyolysis. Age of onset ranged from 12 to 27 years of age (median age: 17 years). There is no family history of myalgia or rhabdomyolysis in any of the families reported in this study. Three of patients were/are elite-level athletes in their chosen fields: Patient FIN1 was a competitive swimmer at a national level, Patient USA1 is an elite high school lacrosse player and Patient UK1 in early adult life competed nationally in the 200 m and 400 m distance races without symptoms. Detailed clinical summaries and investigations are available in the Supplementary material.

The triggers in two cases were exercise and heat (Patients AUS1 and TUR1), in two only exercise (Patients AUS2 and FIN1), in another both episodes occurred following travel (long-haul flight and bus trips; Patient USA1) and in one the episodes occurred spontaneously (Patient UK1). All patients experienced recurrent bouts of rhabdomyolysis (more than two events), with one patient experiencing up to six episodes per year. Peak CK levels ranged from 17 000–603 000 IU/l (median 312 500 U/l). Basal CK ranged between normal to mildly elevated (<1000 IU/l).

Other myopathic features are present between episodes of rhabdomyolysis, including myalgia (5/6), exercise intolerance (3/6) and muscle weakness (1/6). Three of the six probands experienced acute renal failure (Patients AUS1, TUR1 and USA1), in at least one case necessitating kidney dialysis. In two probands, rhabdomyolysis was associated with compartment syndrome (Patients AUS1 and USA1). In Patient AUS1, compartment syndrome involved both lower limbs and required fasciotomy; in Patient USA1 compartment syndrome during two episodes required fasciotomy.

None of the cases presented with cardiac involvement or have developed any symptoms of cardiac disease. There is no history of cardiomyopathy in first degree relatives of the probands.

Patient AUS1 had resting tachycardia post-presentation with rhabdomyolysis but no clear cardiac involvement. He had a normal cardiac MRI and normal echocardiogram. Cardiac investigations were also normal in Patient UK1.

The clinical findings in each of the cases are presented in Table 1 and in the Supplementary material. Lower limb muscle MRI in Patients AUS1 and FIN1 (Supplementary Fig. 1) were normal.

Muscle biopsies were available for review in all cases. The findings on muscle biopsies ranged from within normal limits to non-specific mild myopathic changes and prominent central cores (Fig. 1). Mild subsarcolemmal accumulations of glycogen (Patients FIN1 and USA1), dilated SR and t-tubules (Patient FIN1), mild increase in internal lipid droplets (Patient TUR1), increased variation in myofibre size (Patients AUS1, AUS2, TUR1 and UK1), internal nuclei (Patients AUS1 and TUR1) and central cores in type I myofibres (Patient AUS2).

Genetics

We identified 10 rare or novel bi-allelic loss-of-function variants in *OBSCN* co-segregating with predisposition to rhabdomyolysis in six families (Table 2 and Fig. 2). In Patient AUS1 we identified a homozygous nonsense variant in *OBSCN* [NM_001271223.2 corresponds to the inferred complete (IC) obscurin isoform; exon 62, c.16230C>A, p.(Cys5410*)]. The variant (*rs*1322344930) is present on 4 of 273 940 alleles in gnomAD. The variant was confirmed by bi-directional Sanger sequencing; studies of familial DNA showed that both healthy parents and younger brother were all carriers of the variant. In Patient AUS2 we identified two variants, a nonsense variant in exon 21 [c.6102G>A, p.(Trp2034*)] and an essential splice donor site variant (exon 24, c.7078+1G>T). The nonsense and essential splice-site variants were maternally and paternally inherited, respectively. One of the unaffected sisters (Individual II:4) also harbours bi-allelic *OBSCN* variants. We did not have access to RNA-seq data from Patient AUS2; however, we have data from an unrelated patient that also carries the c.7078+1G>T variant. RNA-seq studies on skeletal muscle found that the main consequence of the c.7078+1G>T variant is skipping of the first two nucleotides of exon 25 (data not shown). Thus, the major consequence of this change is likely a frameshift. Both were rare in gnomAD (allele frequency < 0.0002), with no homozygotes present. Patient FIN1 harboured bi-allelic *OBSCN* deletions; exon36: c.9563_9576del, p.(Leu3188Arg*fs**40) and exon105: c.23385_23386del, p.(Ser7796*). The c.9563_9576del variant is novel, whilst the c.23385_23386del is present on 740 alleles in gnomAD including four homozygote individuals. Three of the four homozygotes are of Finnish background and the allele frequency in Finns is 0.006. In Patient TUR1 a homozygous rare nonsense variant was identified in exon 46 [c.14818C>T, p.(Arg4940*)]. This variant was present on 5 of 209 424 alleles in gnomAD, there were no homozygotes. Sanger sequencing found that each parent carried the variant and that her unaffected brother did not carry the variant. The variant was absent from ~2500 Turkish exomes suggesting that this is not a common variant in the Turkish population. Patient UK1 harboured bi-allelic nonsense variants [exon 31: c.8253G>A, p.(Trp2751*) and exon 42: c.11122A>T, p.(Lys3708*)]. Two healthy siblings had single mono-allelic variants. The c.8253G>A variant is novel and the c.11122A>T variant is present on two alleles in gnomAD. Patient USA1 harboured a multinucleotide variant (MNV) in exon 2, which is annotated as c.386T>A, p.Phe129Tyr (*rs*749567826) and c.387C>A (*rs*769050588), p.Phe129Leu but since they alter the same codon the consequence of these variants is c.386_387delinsAA, p.(Phe129*). This MNV is present on 114 alleles in gnomAD, including two homozygotes. Both homozygotes are within the Ashkenazi Jewish population and the allele frequency in this population is 0.012. The second variant in Patient USA1 occurs at the essential splice donor site of exon 90, c.21532+1G>A; this rare variant is present on three alleles in gnomAD. The exon 90 splice-site variant is inherited maternally and is predicted to result in skipping of exon 90 and a frameshift deletion.

Table 1 Clinical details of six probands with bi-allelic loss-of-function *OBSCN* variants

ID	Age/sex (Age at first episode)	Onset of muscle symptoms and basal neurological examination	Peak CK (IU/l)/ basal CK between episodes	Rhabdo trigger	No. of episodes	Muscle pathology	Acyl carnitine profiles and or ischaemic/non-ischaemic forearm test results	LL Muscle MRI	Cardiac MRI	Exercise intolerance	Myalgia	Muscle weakness	Compartment syndrome	Renal failure
AUS1	20 y/M (18 y)	Exercise-induced myalgia and muscle cramps in childhood, mild distal weakness and exercise intolerance.	> 500 000/ ~200–500	Heat, exercise	2	Mild random variation in myofibre size, increased central nuclei, occasional necrotic and regenerating myofibres present.	Acyl carnitine—normal	Normal	Normal	Y	Y	Y (distal)	Y	Y
AUS2	39 y/M (27 y)	Presented for review after exercise intolerance and rhabdomyolysis. Normal on examination.	275 000/ normal	Exercise	> 2	Central core disease with fibre type variation	Acyl carnitine—normal	N/A	N/A	Y	Y	N	N	N
FIN1	38 y/M (15 y)	Occasional exercise-related myalgias in childhood	> 90 000/ normal-mildy elevated	Exercise	> 2	Glycogen accumulation, dilated SR/T-tubules.	Acyl carnitine—normal	Normal	N/A	N	Y	N	N	N
TUR1	20 y/F (17yo)	Exercise-related myalgia and muscle cramps	> 350 000/ ~400	Heat, exercise	2	Abnormal variation in myofibre size, increased internal nuclei. Some predominance of type 2 myofibres, lobulation of type 1 myofibres, core-like regions.	N/A	N/A	N/A	Y	Y	N	N	Y
UK1	41 y/F (teens)	Recurrent rhabdomyolysis	17 000/ normal	None	Up to 6/y	Within normal limits	Acyl carnitine—normal	Unremarkable	Normal	N	N	N	N	N
USA1	19 y/M (12 y)	Exercise-related myalgia in childhood. Physically very active. Elite high school athlete (lacrosse).	603 000/ 500–1000	None	3	N/A	Acyl carnitine—normal. Baylor metabolomic testing normal. No ischaemic forearm test.	N/A	N/A	N	Y	N	Y	Y

CK = creatine kinase; F = female; LL = lower limb; M = male; N = no; SR/T = sarcoplasmic reticulum/transverse; Y = yes.

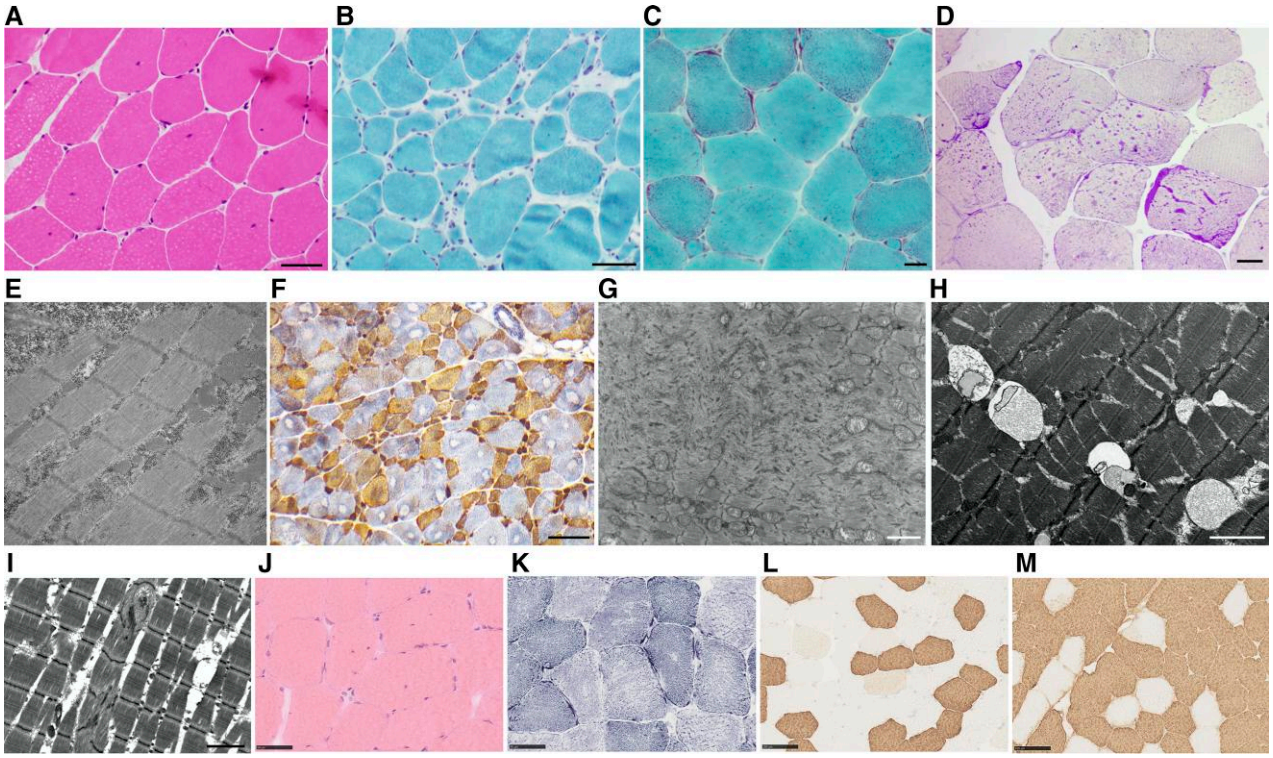

Figure 1 Muscle pathology, by light and electron microscopy (EM), associated with bi-allelic null *OBSCN* variants. Features ranged from within normal limits to mild myopathic changes with increased variation in myofibre size and internal nuclei [(**A**) Patient AUS1 and (**J**) Patient TUR1 (haematoxylin and eosin), (**B**) Patient AUS2 and (**C**) Patient UK1 (Gomori trichrome)]. Glycogen accumulations are evident in skeletal muscle from Patient FIN1 (**D**; periodic acid-Schiff staining) and Patient USA1 (**E**, EM). Prominent central cores are seen in type I myofibres of Patient AUS2 [**F**, NADH(blue)-fast myosin (brown) combined enzyme-immunohistochemistry and **G**, EM]. (**K**) NADH staining on Patient TUR1 shows mild disruption of internal architecture, type I myofibres appear almost lobulated and occasional small core-like areas. Slow (**L**) and fast (**M**) myosin staining in Patient TUR1 shows mild predominance of type II myofibres, type I myofibres relatively small and few intermediate myofibres. Dilated SR and t-tubules are also evident in the muscle biopsy of Patient FIN1 (**H**; EM). Focal Z-band streaming is seen in skeletal muscle from Patient AUS1 (**I**; EM). Scale bars = 20 μm (**C** and **D**), 50 μm (**A**, **B**, **K** and **J**) 100 μm (**F**, **L** and **M**) and 2 μm (**G**, **H** and **I**).

Obscurin exon usage

In skeletal muscle, *OBSCN* encodes two canonical isoforms (A and B); obscurin A (~720 kDa) includes 65 immunoglobin domains and two fibronectin III domains along with a number of C-terminal signalling domains.[40] The larger isoform, obscurin B (~870 kDa), has a similar structure to obscurin A but diverges at the C-terminal region where it contains two Ser/Thr kinase domains.[40] Exons 21 and 105 are annotated in the IC obscurin isoform; however, exon 21 is not present in obscurin A or B and exon 105 is only present in the long isoform (isoform B). To investigate this, we examined exon usage in RNA-seq data from human adult skeletal muscle samples. Exon 21 was present in 93% (80 165 reads supporting the junction between exons 20 and 21) of all transcripts (Fig. 3A). The shorter isoform of obscurin (obscurin A) utilizes an alternative 3′UTR in exon 92. RNA-seq analysis showed that 61% of all transcripts correspond to this short isoform (90 070 reads supporting the inclusion of the exon 92 alternative 3′UTR). There were 39% of reads ($n = 58\,551$) supporting the skipping of the alternative 3′ UTR in exon 92, and accounting for the longer isoform (obscurin B; Fig. 3A).

Similarly, at a protein level, the ratio between obscurin A and B isoforms is almost 50-50 in the adult muscles (Fig. 3C). We therefore conclude, based on knowledge of *OBSCN* expression, that each of the variants identified is predicted to result in loss of a considerable portion of obscurin A and/or B isoforms.

Obscurin transcript and protein levels are reduced in patient skeletal muscle

To determine whether the homozygous AUS1 variant [c.16230C>A, p.(Cys5410*)] was associated with a decrease in *OBSCN* transcript abundance, we performed qPCR using cDNA obtained from patient muscle biopsy and five unrelated control muscle biopsies. The average normalized *OBSCN* transcript abundance of control samples was 11.2-fold greater than in the patient muscle (average normalized OBSCN transcript abundance of 4.25 ± 1.9 in the control, versus 0.38 in the patient; Fig. 3B). To ensure that this difference was specific to *OBSCN* transcript, and not an artefact, we also measured the transcript abundance of three additional genes; ryanodine receptor 1 (*RYR1*), skeletal muscle alpha-actin (*ACTA1*) and myogenin (*MYOG*). For each of these three genes, the transcript abundance measured in the patient sample was within the range of values obtained for the control samples (Fig. 3B). This indicates that the decreased *OBSCN* transcript abundance is likely a real finding.

Western blot performed for obscurin in skeletal muscle from Patients FIN1 and AUS1 showed greatly reduced levels of both isoforms of obscurin (A and B) compared to three healthy control muscle samples (Fig. 3C). In Patient FIN1 there is some retention of obscurin A, this most probably represents obscurin A arising from the allele harbouring the nonsense variant in exon 105 that is excluded in the short isoform A. This suggests that the disease manifests due to reduced levels or absence of obscurin protein in patient

Table 2 Details of the *OBSCN* variants identified in six recurrent rhabdomyolysis probands

Patient	AUS1	AUS2		FIN1	FIN1	TUR1	UK1		USA1	
Variant NM_001271223.2	exon 62: c.16230C>A	exon 21: c.6102G>A	exon 24: c.7078+1G>T	exon36: c.9563_9576del	exon105: c.23385_23386del	exon46: c.14818C>T	exon31: c.8253G>A	exon42: c.11122A>T	exon2: c.386_387delinsAA	exon90: c.21532+1G>A
obscurin isoform IC	p.(Cys5410*)–hmz	p.(Trp2034*)	p.(?)	p.(Leu3188Argfs*40)	p.(Ser7796*)	p.(Arg4940*)–hmz	p.(Trp2751*)	p.(Lys3708*)	p.(Phe129*)	p.(?)
Null in isoform A/B[a]	Y/Y	N/N	Y/Y	Y/Y	N/Y	Y/Y	Y/Y	Y/Y	Y/Y	Y/Y
gnomAD allele frequency	1.46×10^{-5}	1.21×10^{-5}	1.12×10^{-4}	0	3.79×10^{-3}	2.39×10^{-5}	0	8.04×10^{-6}	7.33×10^{-4}	1.58×10^{-5}
gnomAD hmz individuals	0	0	0	0	4	0	0	0	2	0
rs number	rs1322344930	rs775772574	rs200849058	—	rs536227878	rs766814997	—	rs758536677	rs749567826 and rs769050588 (MNV)	rs750494213

Hmz = homozygous; IC = inferred complete isoform; N = no; Y = yes.
[a]OBSCN transcript variant 1, NM_052843.4, obscurin isoform A, OBSCN transcript variant 2, NM_001098623.2, obscurin isoform B.

skeletal muscle. Total loading of muscle protein is indicated by band intensities for other large muscle proteins (titin and nebulin).

Ca^{2+} handling is impaired in cultured patient cells

Ca^{2+} is tightly regulated in skeletal muscle and impairment in Ca^{2+} channel function is a recognised mechanism in rhabdomyolysis. Moreover, obscurin is also thought to be involved in SR function and Ca^{2+} regulation.[27,28] To analyse the SR network, we performed immunolabelling with the antibody anti-calnexin on primary myoblasts from a healthy control and Patient UK1, in growth medium. By confocal microscopy, we did not find any differences in patient myoblasts compared to the control (Fig. 4A), not even after quantification of myoblast total SR nor in other morphological parameters [sphericity, length (Fig. 4B), roundness, elongation and flatness (not shown)].

We studied regulation of SR Ca^{2+} content in myoblasts and found that starvation (EBSS medium) induced a decrease in Ca^{2+} SR content when compared to normal growth conditions (Fig. 4C, $P < 0.001$) probably reflecting lower efficiency when pumping Ca^{2+} back into the SR or a decrease in Ca^{2+} SR storage ability when cell metabolism is diminished. Susceptibility to starvation is exacerbated in Patient UK1 myoblasts as we observed a $69 \pm 6\%$ decrease in Ca^{2+} SR content compared to $33 \pm 2\%$ in control myoblasts (Fig. 4D, $P < 0.001$). This result suggests that patient myoblasts have a decreased ability to fill the SR during starvation conditions for the same reasons as described above. Moreover, obscurin deficiency is associated with greater myoblast death under basal conditions as attested by caspase expression (Fig. 4E, $P < 0.001$). When quantified by flow cytometry, cell death in patient myoblasts was 54% compared to 34% in control myoblasts (Fig. 4F). These data are preliminary and further work is required to confirm these initial findings.

Discussion

Herein we described six patients with susceptibility to severe, recurrent rhabdomyolysis (peak CKs ranged from 17 000–603 000 IU/l) due to bi-allelic loss-of-function variants in *OBSCN*. All cases had experienced at least two episodes of rhabdomyolysis, with one individual (Patient UK1) experiencing up to six episodes per year. Triggers included exercise (including mild exercise, $n = 4$) and heat ($n = 2$); in two individuals the episodes occur without obvious triggers.

In most cases there was a prior history of myalgia and muscle cramps. Basal CK between episodes ranged from normal to mildly elevated (< 1000 IU/l). Three patients were/are elite level athletes in their chosen fields. Elite athletic performance preceding the onset of neuromuscular disease has been noted anecdotally for other genetic neuromuscular diseases; most notably in patients with pathogenic variants in *ANO5*, *CAPN3*, *CAV3*, *DYSF* and *RYR1*.[3,14,41–44]

One sibling (Individual II:4) in Family AUS2 also harbours bi-allelic *OBSCN* variants but has not had rhabdomyolysis. She is awaiting formal assessment by a neurologist. This is in keeping with rhabdomyolysis requiring an underlying genetic factor in combination with environmental triggers. Individual II:4 is not active, as the proband is, and thus it is likely that her levels of physical activity have been insufficient to trigger a rhabdomyolysis event. There may also be other factors contributing to rhabdomyolysis, for example rhabdomyolysis is recognised to occur more frequently in males. There are many individuals in gnomAD that carry well established pathogenic variants underlying exertional

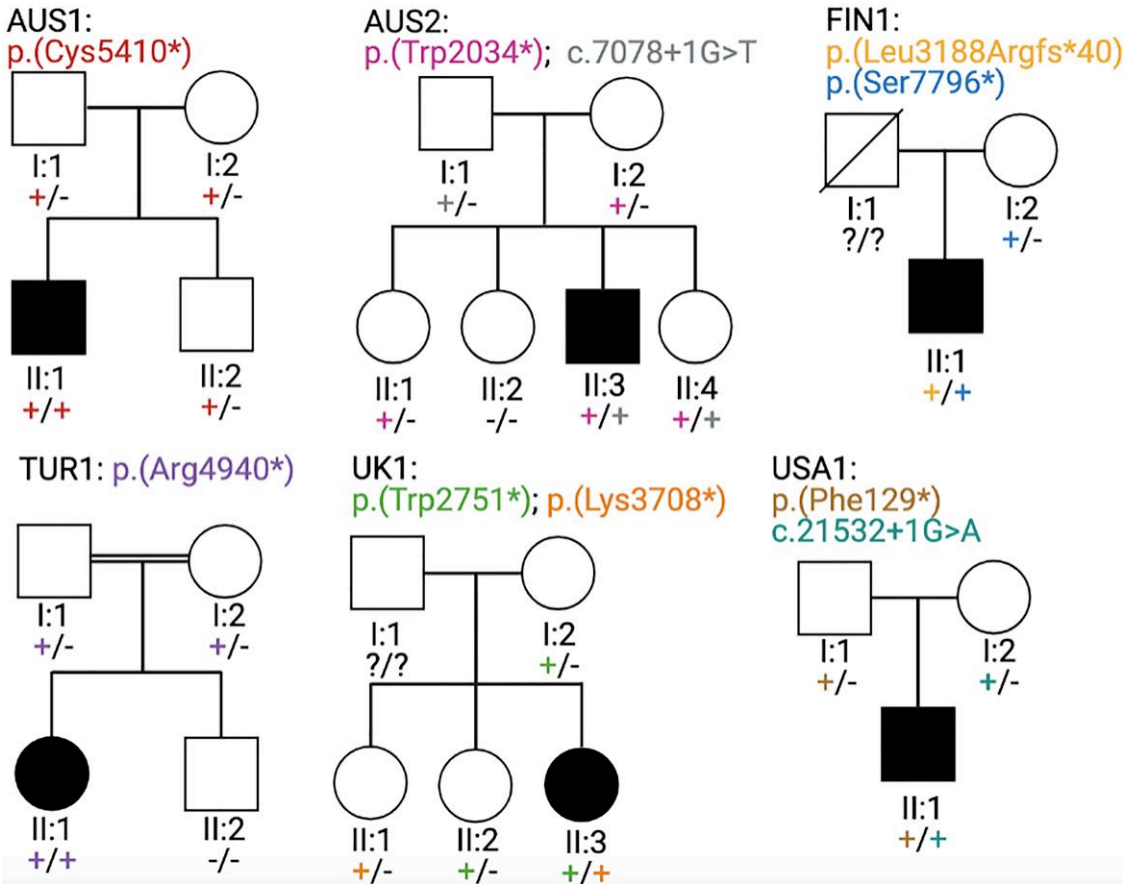

Figure 2 Pedigrees for the six families segregating bi-allelic loss-of-function variants in *OBSCN* with predisposition to recurrent rhabdomyolysis.

rhabdomyolysis, hyper CK and malignant hyperthermia. These include individuals homozygous for the most common *CPT2* (p.Ser116Leu, $n = 4$) and *ANO5* (p.Asn64Lys*fs**15, $n = 2$) variants and individuals heterozygous for known pathogenic dominantly-inherited RYR1 variants ($n = 3$–30 per variant). Together, these data suggest that bi-allelic loss-of-function *OBSCN* variants are in some instances insufficient on their own to precipitate rhabdomyolysis.

Features on muscle biopsy ranged from unremarkable and minimal non-specific changes through to striking central cores in type I myofibres. Increased internal nuclei, mild variation in myofibre size and glycogen accumulations were each reported in more than one case. Other features included increased lipid droplets, core-like regions, type II myofibre predominance and occasional myofibre atrophy and nuclear clumps. Cores have been observed in patients with rhabdomyolysis and likely pathogenic variants in genes encoding components of the Ca^{2+} signalling pathway (*RYR1* and *CACNA1S*).[3,45] Aberrant Ca^{2+} handling was observed in Patient UK1 myoblasts, thus altered Ca^{2+} signalling may represented a unifying mechanism in the development of cores and rhabdomyolysis in patients with *RYR1*, *CACNA1S* and *OBSCN* variants.

Population variant frequency data show that all loss-of-function variants for which there are homozygous individuals in gnomAD are flagged as a MNV (which together do not result in loss-of-function changes at the amino acid level) or have loss-of-function curation notes of 'uncertain' or 'not loss-of-function (LOF)' (Supplementary Fig. 2). This suggests that bi-allelic loss-of-function variants in *OBSCN* are likely to be pathogenic. This association was perhaps delayed due to the presence of a relatively common spurious loss-of-function variant in *OBSCN* [p.Arg3252* (AGA > TGA), *rs*3795786, allele frequency: 0.03, gnomAD: >900 homozygote individuals]. However, this variant was subsequently annotated as a MNV associated with a protein change of p.Arg3252Leu (AGA > TTA). One of the variants [p.(Ser7796*)] we identified in exon 105 is present in four individuals in the homozygous state in gnomAD and is present on one allele in FIN1. This annotation of 'uncertain' is likely due to this exon not being predicted to cause a null allele in OBSCN isoform A. However, this exon is expressed at similar levels to flanking exons that are present in the long isoform. Furthermore, by western blot we have shown a reduction of OBSCN isoform A and B in Patient FIN1 skeletal muscle.

Two variants reported in this cohort are present in ~1% of individuals in specific control populations. The MNV [c.386_387delinsAA, p.(Phe129*)] identified in Patient USA1 is present at an allele frequency of 0.012 in individuals of Ashkenazi Jewish ancestry (0.0007 in the total population) and there are two homozygous Ashkenazi Jewish individuals in gnomAD. The p.(Ser7796*) variant present in FIN1 is present at an allele frequency of 0.009 in the Finnish population in gnomAD and 0.0038 in the total population. Thus, these variants may predispose individuals within these populations to rhabdomyolysis.

The finding of similar expression of exons not thought to be included in 'canonical' functional isoforms of *OBSCN* is similar to the identification of exons within *TTN* that were thought to only occur in the meta-transcript but were later shown to be present in *TTN* transcripts in adult skeletal muscle.[46] Our findings suggest that further studies are needed to provide a

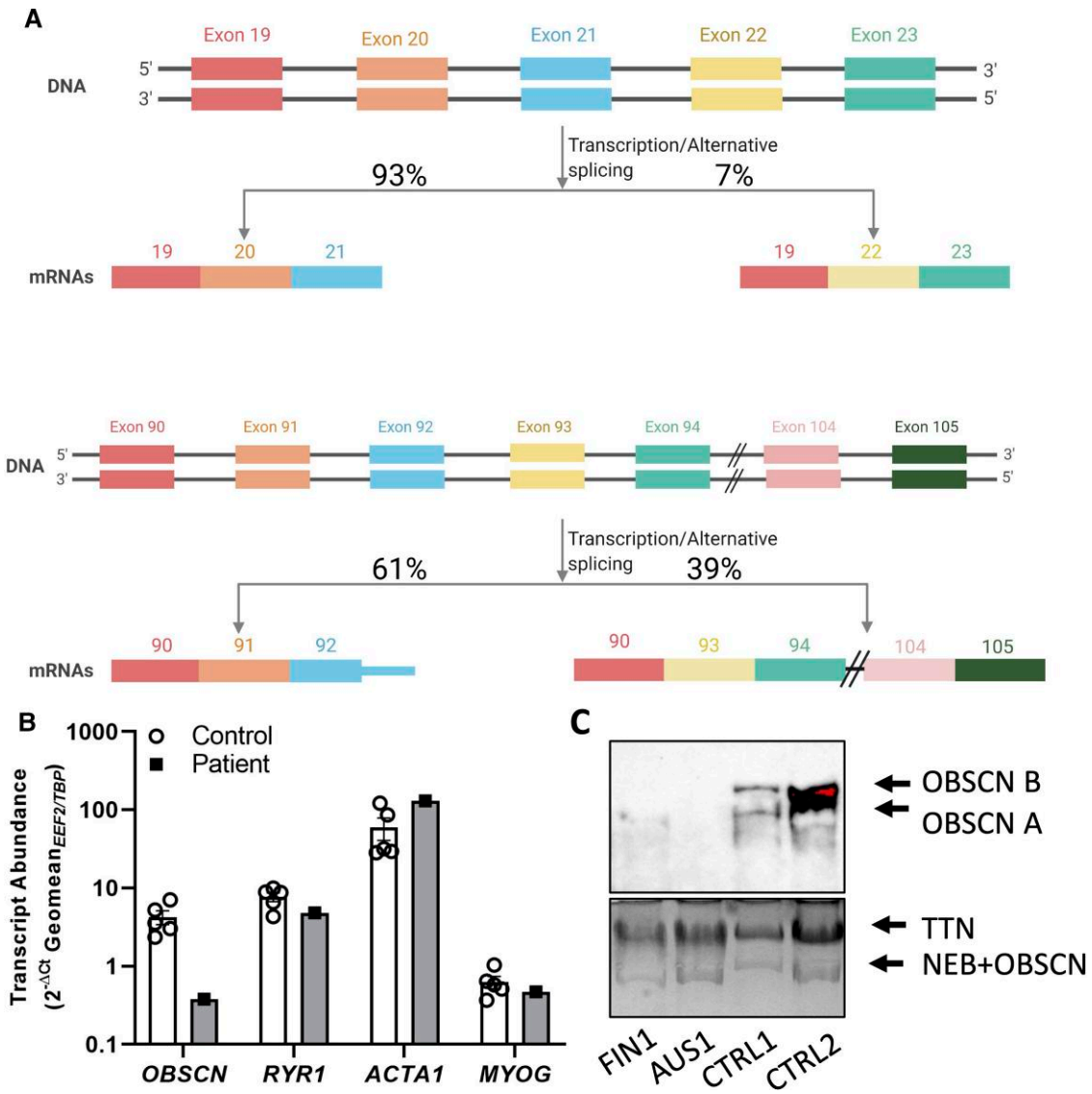

Figure 3 Obscurin transcript and protein abundance in healthy control and patient skeletal muscle. (**A**) A schematic showing exon usage of exons 21 and 105, generated from skeletal muscle RNA-seq data. (**B**) Transcript abundance of *OBSCN*, *RYR1*, *ACTA1* and *MYOG* in human skeletal muscle obtained from the patient (filled square, grey bars) and five unrelated controls (open circles, white bars) was assessed by qPCR. *OBSCN* transcript abundance is specifically reduced by more than 10-fold in Patient AUS1 skeletal muscle relative to controls. Expression of each transcript was normalized to the geometric mean of two endogenous control genes (*EEF2* and *TBP*) using the delta Ct method. Graphed data represent the mean ± SEM. (**C**) Western blot showing reduction/absence of OBSCN in patient muscle (Patients FIN1 and AUS1) compared to healthy control (CTRL) samples. Coomassie staining of the TTN and NEB protein bands are shown to demonstrate loading of total muscle protein.

comprehensive picture of the complex *OBSCN* splicing pattern. As already demonstrated with the even larger *TTN* transcripts, this is crucial for a proper clinical interpretation of variants in such large genes.[47]

Obscurin was originally identified as a titin-binding protein and has been observed to localize to the M-band and also the Z-disk of striated muscle.[25] At the M-band, obscurin interactions with titin, myomesin and myosin binding protein C. Binding at the titin C-termins Ig domain (M10) is responsible for the predominant M-band localization in mature myofilaments. Heterozygous variants in the titin M10 domain cause dominant tibial muscular dystrophy (TMD)[48] and bi-allelic variants cause LGMD R10.[49] These variants disrupt binding with obscurin. TMD variants associated with different clinical severity, correlate with the degree of loss of obscurin interaction.[25]

Obscurin's precise role in skeletal muscle development, function and disease has remained obscure.[50] It had been shown in *Caenorhabditis elegans*, *Drosophila melanogaster* and *Danio rerio* that obscurin and its homologue unc-89 might play an important role in sarcomerogenesis and the lateral alignment of sarcomeres.[51–53]

Four obscurin isoforms have been characterised, including two high molecular weight proteins (obscurin A and B) that are abundant in skeletal muscle.[28] Obscurin A contains two COOH-terminal binding sites that can interact with ankyrin proteins,[54] including small ankyrin 1 (sAnk1.5) of the SR. Obscurin is thus proposed to play a key role linking the contractile apparatus to the SR. *Obscn* null[27] and *sAnk1.5* null[55] mice both show reduced longitudinal SR volume. Muscle from Patient FIN1 showed markedly dilated t-tubules by electron microscopy, this may indicate that the SR is impaired in obscurin-related myopathy.

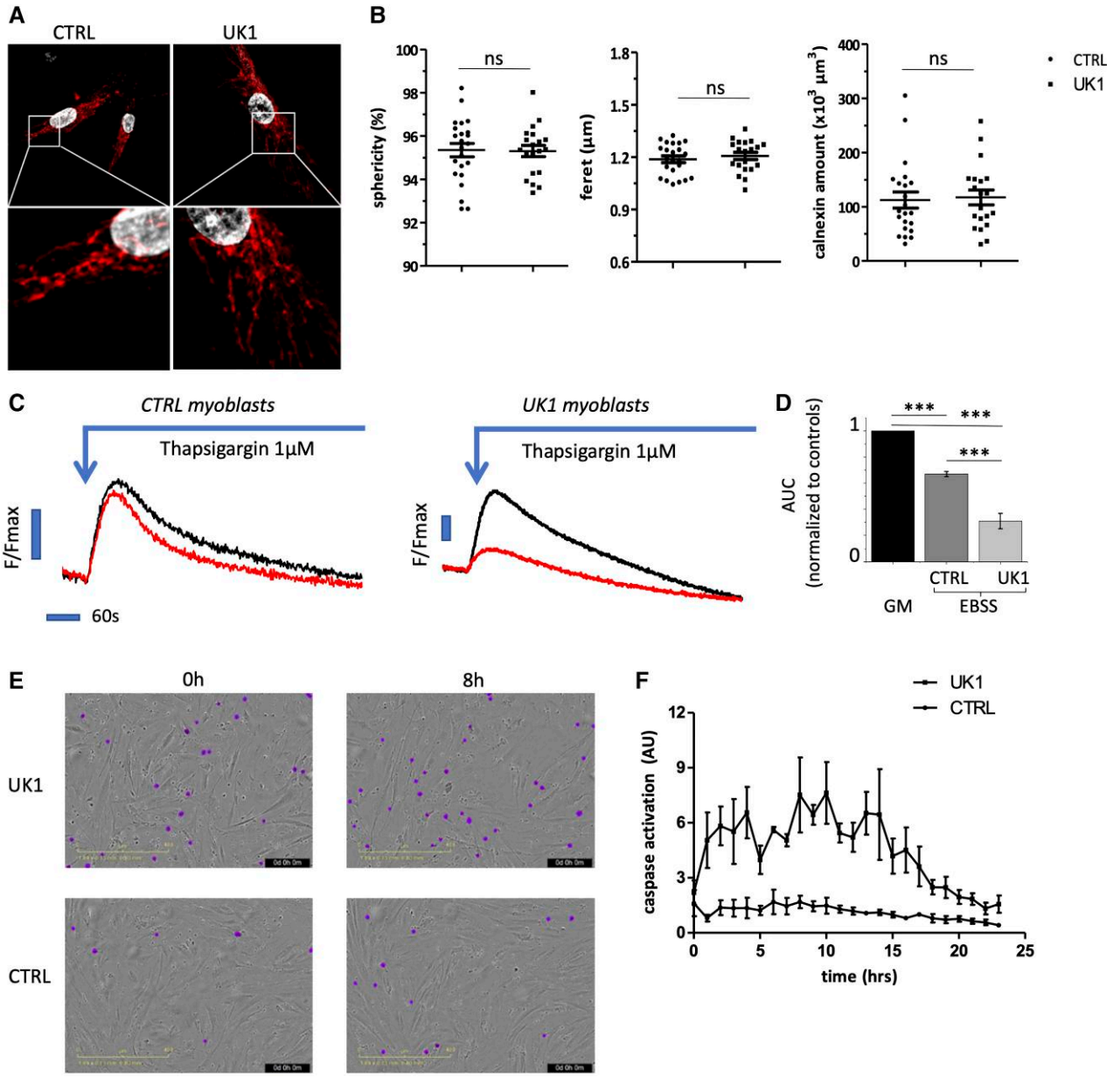

Figure 4 Studies from patient (Patient UK1) myoblasts show aberrant Ca^{2+} flux and increased cell death. (**A**) SR morphology is not altered in patient myoblasts when compared to control myoblasts as shown by immunostaining with anti-calnexin antibody and confocal analysis. (**B**) Total SR content and the morphological parameters measured (length, sphericity) are similar in healthy control (CTRL) and patient myoblasts. (**C**) Representative SR Ca^{2+} content measurements in myoblasts from a healthy control (CTRL, *left*) and patient (*right*) in control (GM, black traces) and EBSS medium for 2 h (red traces). (**D**) SR Ca^{2+} content was assessed from the area under the curves (AUC) after thapsigargin addition. Horizontal bar, 0 s; vertical bars F/Fmax 0.1 (arbitrary units). Histograms summarizing AUC in control (GM) and EBSS media. Data from 12 and six individual wells for CTRL and patient, respectively obtained from two independent experiments corresponding to a decrease of 33 ± 2% (CTRL) and 69 ± 6% (Patient) of SR Ca^{2+} contents in EBSS medium. (**E**) Apoptosis was assessed from purple events representing caspase 3/7 positive cells normalised to cell number. Patient myoblasts show higher levels of apoptosis (2.3-fold) as detected by caspase 3/7 expression when compared to CRTL myoblasts. (**F**) Quantification of caspase 3/7 expression in control and patient myoblasts. Results of one representative experiment out of two independent experiments.

Despite the great variability of causes, genetic or otherwise, rhabdomyolysis is thought to have the same downstream mechanism. Shortage of energy results in pump dysfunction (Na/K-ATPase, Ca^{2+} ATPase pump), which leads to increased cellular permeability to Na^{+} and an increased intracellular Ca^{2+} concentration.[56] High intracellular Ca^{2+} levels enhance the activation of Ca^{2+}-dependent proteases and phospholipases, which contribute to the destruction of myofibrillar, cytoskeletal, and membrane proteins and leakage of myofibre contents, such as electrolytes, creatine kinase and myoglobin, into the circulation.[57] Aberrant Ca^{2+} flux into cytosol and cell death are the hallmarks of rhabdomyolysis.[58] SR Ca^{2+} contents are likely to be affected in rhabdomyolysis. In fact, SR Ca^{2+} contents depletion, may reflect a lower level of SERCA activity and/or an increased Ca^{2+} leak and this has two major consequences. Firstly, skeletal muscle contraction mainly relies on the amount of Ca^{2+} released from SR and, as observed in heart failure,[59,60] a decrease in

SR Ca^{2+} contents is associated with smaller amplitude and slower kinetics in cytosolic Ca^{2+} transients as well as slower SR Ca^{2+} reuptake. Therefore, repetitive muscle contractions in patients with rhabdomyolysis may lead to rapid exhaustion due to reduced SR Ca^{2+} contents as well as slower kinetics of Ca^{2+} release and repumping. Secondly, decreased SR contents is associated with stress disturbing folding of proteins related to the adaptative mechanism called the unfolded protein response (UPR) aimed to clear unfolded proteins and restore SR homeostasis.[61] SR stress often promotes apoptosis and lead to cell death as observed in rhabdomyolysis patients. Study of *OBSCN* null cell-lines (derived from mouse models, knock-down of *OBSCN* or patients), are now needed to strengthen these observations, including restoration of normal SERCA activity and measurements of Ca^{2+} signals in skeletal muscle during repetitive electrical stimulation.

Studies by Lange and colleagues of *Obscn* null mice failed to identify any defects in sarcomere structure and alignment.[27,28] In contrast, Sorrentino's team also generated and studied *Obscn* null mice, and found defects in sarcolemmal integrity and muscle damage in response to exercise.[29,30] No defects suggestive of rhabdomyolysis or impaired Ca^{2+} handling were noted in these mice studies; however it is tempting to postulate that muscle damage triggered by obscurin deficiency, may lead to rhabdomyolysis susceptibility. Indeed, four of our six patients experienced rhabdomyolysis following exercise, in some instances mild exercise was sufficient to trigger an episode, i.e. climbing a flight of stairs. In the future, it may be of interest to explore the susceptibility of *Obscn* null mice to exercise and/or heat-induced muscle damage.

Our patients are relatively young, it will be interesting to follow up this cohort and identify additional cases with obscurin deficiency to determine the natural history and progression of the disease into later life.

Heterozygous variants (missense, splice-site and frameshift) in *OBSCN* have been associated with cardiomyopathy (dilated cardiomyopathy, hypertrophic cardiomyopathy, left ventricular non-compaction) in patients.[40,62,63] However, as highlighted in Grogan and Kontrogianni-Konstantopoulos the functional consequences of the identified *OBSCN* variants remain elusive.[64] More recently, a study by Fukuzuwa *et al*. has provided compelling evidence against the pathogenicity of one of the more widely-studied *OBSCN* variants (p.Arg4344Gln).[65] This study found no functional deficits associated with this variant (including studies to assess protein-protein interactions and thermostability).[65] In addition, 15% of African Americans were noted to carry this variant.[65] *Obscn*$^{-/-}$ mice do not exhibit any signs of cardiomyopathy.[27] In GTEx, *OBSCN* is highly enriched in skeletal muscle (median TPM 213) compared to all other tissues and is expressed at much lower levels in the heart (left ventricle: median TPM 35, atria appendage: median TPM 24; https://www.gtexportal.org/home/gene/OBSCN). In a systematic review of cardiomyopathy genetics, Ingles *et al*. classified the association between *OBSCN* variants and dilated cardiomyopathy as 'limited' based on the available literature and scientific evidence.[66] None of the patients in this cohort nor any of their carrier first-degree relatives report any cardiac involvement, suggesting that loss-of-function *OBSCN* variants are unlikely to represent a substantial cause of cardiomyopathy.

In summary, we have identified bi-allelic loss-of-function variants in *OBSCN* predisposing individuals to recurrent rhabdomyolysis, typically presenting in teenage years. *OBSCN* should be considered in the genetic diagnosis of rhabdomyolysis.

Acknowledgements

The authors thank the patients and their families for participating in this study. We also thank Nicolas Goudin and Meriem Garfa from the cell-imaging platform; the Oxford Genomics Centre at the Wellcome Centre for Human Genetics (funded by Welcome Trust grant reference 203141/Z/16/Z) for the generation and initial processing of the RNA sequencing data.

Funding

This work is supported by Australian National Health and Medical Research Council (NHMRC) grants (APP1080587, APP1146321 and APP2002640) to G.R., A.R.R.F. and N.G.L. G.R. is supported by an NHMRC Career Development Fellowship (APP1122952) and N.G.L. and A.R.R.F. are supported by NHMRC Senior Research Fellowships (APP1117510, APP1154524). This work was also supported by the Academy of Finland Neurogenomics pHealth funding. This work was supported by grants to PdL from Fondation maladies rares, Agence Nationale de la Recherche (ANR – AAPG 2018 CE17 MetabInf), the Association Française contre les Myopathies (AFM 2016–2018 19773), and patient associations (Nos Anges, AMMI, OPPH, TANGO2 family associations, Hyperinsulinisme).

Competing interests

The authors report no competing interests.

Supplementary material

Supplementary material is available at *Brain* online.

References

1. Stahl K, Rastelli E, Schoser B. A systematic review on the definition of rhabdomyolysis. *J Neurol*. 2020;267:877–882.
2. Kenney K, Landau ME, Gonzalez RS, Hundertmark J, O'Brien K, Campbell WW. Serum creatine kinase after exercise: drawing the line between physiological response and exertional rhabdomyolysis. *Muscle Nerve*. 2012;45:356–362.
3. Scalco RS, Gardiner AR, Pitceathly RD, et al. Rhabdomyolysis: a genetic perspective. *Orphanet J Rare Dis*. 2015;10:51.
4. Aleckovic-Halilovic M, Pjanic M, Mesic E, Storrar J, Woywodt A. From quail to earthquakes and human conflict: a historical perspective of rhabdomyolysis. *Clin Kidney J*. 2021;14:1088–1096.
5. Kruijt N, van den Bersselaar LR, Kamsteeg EJ, et al. The etiology of rhabdomyolysis: an interaction between genetic susceptibility and external triggers. *Eur J Neurol*. 2021;28:647–659.
6. Orngreen MC, Vissing J. Chapter 29–Metabolic myopathies. In: Hilton-Jones D, ed. *Oxford Textbook of Neuromuscular Disorders*, 2014.
7. Michot C, Hubert L, Romero NB, et al. Study of LPIN1, LPIN2 and LPIN3 in rhabdomyolysis and exercise-induced myalgia. *J Inherit Metab Dis*. 2012;35:1119–1128.
8. Bergounioux J, Brassier A, Rambaud C, et al. Fatal rhabdomyolysis in 2 children with LPIN1 mutations. *J Pediatr*. 2012;160:1052–1054.
9. Lopes Abath Neto O, Medne L, Donkervoort S, et al. MLIP causes recessive myopathy with rhabdomyolysis, myalgia and baseline elevated serum creatine kinase. *Brain*. 2021;144:2722–2731.

10. Alsaif HS, Alshehri A, Sulaiman RA, et al. MYH1 is a candidate gene for recurrent rhabdomyolysis in humans. *Am J Med Genet A*. 2021;185(7):2131–2135.
11. Valberg SJ, Henry ML, Perumbakkam S, Gardner KL, Finno CJ. An E321G MYH1 mutation is strongly associated with nonexertional rhabdomyolysis in Quarter Horses. *J Vet Intern Med*. 2018;32:1718–1725.
12. Mathews KD, Stephan CM, Laubenthal K, et al. Myoglobinuria and muscle pain are common in patients with limb-girdle muscular dystrophy 2I. *Neurology*. 2011;76:194–195.
13. Tarnopolsky M, Hoffman E, Giri M, Shoffner J, Brady L. Alpha-sarcoglycanopathy presenting as exercise intolerance and rhabdomyolysis in two adults. *Neuromuscul Disord*. 2015; 25:952–954.
14. Scalco RS, Gardiner AR, Pitceathly RD, et al. CAV3 mutations causing exercise intolerance, myalgia and rhabdomyolysis: Expanding the phenotypic spectrum of caveolinopathies. *Neuromuscul Disord*. 2016;26:504–510.
15. Lahoria R, Winder TL, Lui J, Al-Owain MA, Milone M. Novel ANO5 homozygous microdeletion causing myalgia and unprovoked rhabdomyolysis in an Arabic man. *Muscle Nerve*. 2014; 50:610–613.
16. Witting N, Laforet P, Voermans NC, et al. Phenotype and genotype of muscle ryanodine receptor rhabdomyolysis-myalgia syndrome. *Acta Neurol Scand*. 2018;137:452–461.
17. Knuiman GJ, Kusters B, Eshuis L, et al. The histopathological spectrum of malignant hyperthermia and rhabdomyolysis due to RYR1 mutations. *J Neurol*. 2019;266:876–887.
18. Gardner L, Miller DM, Daly C, et al. Investigating the genetic susceptibility to exertional heat illness. *J Med Genet*. 2020;57:531–541.
19. Vivante A, Ityel H, Pode-Shakked B, et al. Exome sequencing in Jewish and Arab patients with rhabdomyolysis reveals single-gene etiology in 43% of cases. *Pediatr Nephrol*. 2017;32:2273–2282.
20. Wu L, Brady L, Shoffner J, Tarnopolsky MA. Next-generation sequencing to diagnose muscular dystrophy, rhabdomyolysis, and hyperCKemia. *Can J Neurol Sci*. 2018;45:262–268.
21. Rubegni A, Malandrini A, Dosi C, et al. Next–generation sequencing approach to hyperCKemia: A 2-year cohort study. *Neurol Genet*. 2019;5:e352.
22. Beecroft SJ, Yau KS, Allcock RJN, et al. Targeted gene panel use in 2249 neuromuscular patients: the Australasian referral center experience. *Ann Clin Transl Neurol*. 2020;7:353–362.
23. Bang ML, Centner T, Fornoff F, et al. The complete gene sequence of titin, expression of an unusual approximately 700-kDa titin isoform, and its interaction with obscurin identify a novel Z-line to I-band linking system. *Circ Res*. 2001;89:1065–1072.
24. Fukuzawa A, Idowu S, Gautel M. Complete human gene structure of obscurin: implications for isoform generation by differential splicing. *J Muscle Res Cell Motil*. 2005;26:427–434.
25. Fukuzawa A, Lange S, Holt M, et al. Interactions with titin and myomesin target obscurin and obscurin-like 1 to the M-band: implications for hereditary myopathies. *J Cell Sci*. 2008;121:1841–1851.
26. Kontrogianni-Konstantopoulos A, Ackermann MA, Bowman AL, Yap SV, Bloch RJ. Muscle giants: molecular scaffolds in sarcomerogenesis. *Physiol Rev*. 2009;89:1217–1267.
27. Lange S, Ouyang K, Meyer G, et al. Obscurin determines the architecture of the longitudinal sarcoplasmic reticulum. *J Cell Sci*. 2009;122:2640–2650.
28. Blondelle J, Marrocco V, Clark M, et al. Murine obscurin and Obsl1 have functionally redundant roles in sarcolemmal integrity, sarcoplasmic reticulum organization, and muscle metabolism. *Commun Biol*. 2019;2178.
29. Randazzo D, Giacomello E, Lorenzini S, et al. Obscurin is required for ankyrinB-dependent dystrophin localization and sarcolemma integrity. *J Cell Biol*. 2013;200:523–536.
30. Randazzo D, Blaauw B, Paolini C, et al. Exercise-induced alterations and loss of sarcomeric M-line organization in the diaphragm muscle of obscurin knockout mice. *Am J Physiol Cell Physiol*. 2017;312:C16–C28.
31. Knochel JP, Moore GE. Rhabdomyolysis in Malaria. *N Engl J Med*. 1993;329:1206–1207.
32. Renner C, Razeghi S, Richter T, Ueberall MA, Schless A. Metab-L: an electronic mailing list on inborn errors of metabolism. *Acta Paediatr*. 1997;86:892–894.
33. Dubowitz V, Sewry CA, Oldfors A, eds. *Muscle Biopsy: a practical approach*. 4th ed. Elsevier Limited; 2013.
34. Sainio MT, Valipakka S, Rinaldi B, et al. Recessive PYROXD1 mutations cause adult-onset limb-girdle-type muscular dystrophy. *J Neurol*. 2019;266:353–360.
35. Evilä A, Arumilli M, Udd B, Hackman P. Targeted next-generation sequencing assay for detection of mutations in primary myopathies. *Neuromuscul Disord*. 2016; 26:7–15.
36. Soreze Y, Boutron A, Habarou F, et al. Mutations in human lipoyltransferase gene LIPT1 cause a Leigh disease with secondary deficiency for pyruvate and alpha-ketoglutarate dehydrogenase. *Orphanet J Rare Dis*. 2013;8192.
37. Uapinyoying P, Goecks J, Knoblach SM, et al. A long-read RNA-seq approach to identify novel transcripts of very large genes. *Genome Res*. 2020;30:885–897.
38. Sagath L, Lehtokari VL, Valipakka S, et al. Congenital asymmetric distal myopathy with hemifacial weakness caused by a heterozygous large de novo mosaic deletion in nebulin. *Neuromuscul Disord*. 2021;31(6):539–545.
39. Michot C, Mamoune A, Vamecq J, et al. Combination of lipid metabolism alterations and their sensitivity to inflammatory cytokines in human lipin-1-deficient myoblasts. *Biochim Biophys Acta*. 2013;1832:2103–2114.
40. Grogan A, Tsakiroglou P, Kontrogianni-Konstantopoulos A. Double the trouble: giant proteins with dual kinase activity in the heart. *Biophys Rev*. 2020;12:1019–1029.
41. Bushby KM. Making sense of the limb-girdle muscular dystrophies. *Brain*. 1999;122 (Pt 8):1403–1420.
42. Klinge L, Aboumousa A, Eagle M, et al. New aspects on patients affected by dysferlin deficient muscular dystrophy. *J Neurol Neurosurg Psychiatry*. 2010;81:946–953.
43. Jungbluth H, Dowling JJ, Ferreiro A, Muntoni F, Consortium RYRM. 217th ENMC International Workshop: RYR1-related myopathies, Naarden. The Netherlands:29–31. January 2016. *Neuromuscul Disord*. 2016;26:624–633.
44. Blackburn PR, Selcen D, Jackson JL, et al. Early-onset limb-girdle muscular dystrophy-2L in a female athlete. *Muscle Nerve*. 2017; 55:E19–E21.
45. Anandan C, Cipriani MA, Laughlin RS, Niu Z, Milone M. Rhabdomyolysis and fluctuating asymptomatic hyperCKemia associated with CACNA1S variant. *Eur J Neurol*. 2018;25: 417–419.
46. Oates EC, Jones KJ, Donkervoort S, et al. Congenital Titinopathy: Comprehensive characterization and pathogenic insights. *Ann Neurol*. 2018;83:1105–1124.
47. Savarese M, Jonson PH, Huovinen S, et al. The complexity of titin splicing pattern in human adult skeletal muscles. *Skelet Muscle*. 2018;8:11.
48. Hackman P, Vihola A, Haravuori H, et al. Tibial muscular dystrophy is a titinopathy caused by mutations in TTN, the gene encoding the giant skeletal-muscle protein titin. *Am J Hum Genet*. 2002;71:492–500.
49. Evilä A, Palmio J, Vihola A, et al. Targeted next-generation sequencing reveals novel TTN mutations causing recessive distal titinopathy. *Mol Neurobiol*. 2017;54:7212–7223.

50. Fleming JR, Rani A, Kraft J, Zenker S, Börgeson E, Lange S. Exploring obscurin and SPEG kinase biology. *J Clin Med*. 2021; 10:984.
51. Small TM, Gernert KM, Flaherty DB, Mercer KB, Borodovsky M, Benian GM. Three new isoforms of Caenorhabditis elegans UNC-89 containing MLCK-like protein kinase domains. *J Mol Biol*. 2004;342:91–108.
52. Raeker MO, Su F, Geisler SB, et al. Obscurin is required for the lateral alignment of striated myofibrils in zebrafish. *Dev Dyn*. 2006;235:2018–2029.
53. Katzemich A, Kreiskother N, Alexandrovich A, et al. The function of the M-line protein obscurin in controlling the symmetry of the sarcomere in the flight muscle of Drosophila. *J Cell Sci*. 2012;125:3367–3379.
54. Bagnato P, Barone V, Giacomello E, Rossi D, Sorrentino V. Binding of an ankyrin-1 isoform to obscurin suggests a molecular link between the sarcoplasmic reticulum and myofibrils in striated muscles. *J Cell Biol*. 2003;160:245–253.
55. Giacomello E, Quarta M, Paolini C, et al. Deletion of small ankyrin 1 (sAnk1) isoforms results in structural and functional alterations in aging skeletal muscle fibers. *Am J Physiol Cell Physiol*. 2015;308:C123–C138.
56. Shapiro ML, Baldea A, Luchette FA. Rhabdomyolysis in the intensive care unit. *J Intensive Care Med*. 2012;27:335–342.
57. Torres PA, Helmstetter JA, Kaye AM, Kaye AD. Rhabdomyolysis: pathogenesis, diagnosis, and treatment. *Ochsner J*. 2015;15: 58–69.
58. Knochel JP. Mechanisms of rhabdomyolysis. *Curr Opin Rheumatol*. 1993;5:725–731.
59. Jiang MT, Lokuta AJ, Farrell EF, Wolff MR, Haworth RA, Valdivia HH. Abnormal Ca^{2+} release, but normal ryanodine receptors, in canine and human heart failure. *Circ Res*. 2002;91:1015–1022.
60. Belevych A, Kubalova Z, Terentyev D, Hamlin RL, Carnes CA, Györke S. Enhanced ryanodine receptor-mediated calcium leak determines reduced sarcoplasmic reticulum calcium content in chronic canine heart failure. *Biophys J*. 2007;93:4083–4092.
61. Sano R, Reed JC. ER stress-induced cell death mechanisms. *Biochim Biophys Acta*. 2013;1833:3460–3470.
62. Arimura T, Matsumoto Y, Okazaki O, et al. Structural analysis of obscurin gene in hypertrophic cardiomyopathy. *Biochem Biophys Res Commun*. 2007;362:281–287.
63. Marston S, Montgiraud C, Munster AB, et al. OBSCN Mutations Associated with Dilated Cardiomyopathy and Haploinsufficiency. *PLoS One*. 2015;10:e0138568.
64. Grogan A, Kontrogianni-Konstantopoulos A. Unraveling obscurins in heart disease. *Pflugers Arch*. 2019;471:735–743.
65. Fukuzawa A, Koch D, Grover S, Rees M, Gautel M. When is an obscurin variant pathogenic? The impact of Ar:g4344G. ln and Arg4444Trp variants on protein-protein interactions and protein stability. *Hum Mol Genet*. 2021;30:1131–1141.
66. Ingles J, Goldstein J, Thaxton C, et al. Evaluating the clinical validity of hypertrophic cardiomyopathy genes. *Circ Genom Precis Med*. 2019;12:e002460.